ELSEVIER

Journal of Molecular Catalysis A: Chemical 162 (2000) 297–306

JOURNAL OF MOLECULAR CATALYSIS A: CHEMICAL

www.elsevier.com/locate/molcata

Structural changes of the Cu surface of a $Cu/ZnO/Al_2O_3$ catalyst, resulting from oxidation and reduction, probed by CO infrared spectroscopy

B.H. Sakakini [a], J. Tabatabaei [a], M.J. Watson [b], K.C. Waugh [a,*]

[a] *Department of Chemistry, Faraday Building, UMIST, PO Box 88, Manchester, M60 1QD UK*
[b] *ICI Synetix RT&E, PO Box 1, Billingham, Cleveland, UK*

Abstract

The morphology of the Cu surface of a $Cu/ZnO/Al_2O_3$ (60:30:10) catalyst, produced by reduction of the copper oxide component of the catalyst either with H_2 or CO, has been probed by measuring the IR spectra of CO adsorbed on these surfaces. Pre-reduction in H_2 produces a Cu surface, which contains the (110) and (211) faces and which is active in CO_2 decomposition. Re-reduction of the CO_2-oxidised Cu surface in CO results in a twofold increase in the Cu(211) surface. Re-reduction of the CO_2-oxidised Cu surface in H_2 results in the restoration of the original Cu morphology, i.e. in a decrease in the Cu(211) surface population. Initial reduction of the copper oxide component of the $Cu/ZnO/Al_2O_3$ catalyst by CO produces a surface, which is inactive in the decomposition of CO_2.

Keywords: Copper; Catalyst; Morphology reconstruction; Infrared; Adsorption

1. Introduction

Whether a given heterogeneously catalysed reaction is structure sensitive or not is extremely important to the catalytic industry. This importance was demonstrated in a seminal paper by Hadden et al. [1]. They produced two series of $Cu/ZnO/Al_2O_3$ catalysts of different copper loadings by precipitating one series at a given pH and a second series at a higher pH. They tested these catalysts in the shift reaction and found two distinct linear relationships between the activity in the shift reaction and the copper metal area. The specific activity of the series of catalyst produced at the lower pH was twice that of the series produced at the higher pH. The reaction is obviously structure sensitive, but no method currently exists which could identify the source of the activity in this reaction.

Single crystal studies have shown that, to some extent, the interactions of all of the components of the shift reaction

$$CO + H_2O \leftrightarrow CO_2 + H_2$$

with copper are structure sensitive. Since the shift reaction is run industrially at equilibrium, the interaction of the components of the reverse reaction with copper must also be considered.

* Corresponding author. Tel.: +44-161-200-4503; fax: +44-161-200-4430.
E-mail address: ken.waugh@umist.ac.uk (K.C. Waugh).

1381-1169/00/$ - see front matter
PII: S1381-1169(00)00298-3

2. The adsorption of CO on Cu single crystals and on supported Cu catalysts

While the adsorption of CO on Cu is not activated, its heat of adsorption shows a weak structure dependence having low coverage values between 44 and 50 kJ mol^{-1} on Cu(111) [2,3], between 53 and 60 kJ mol^{-1} on Cu(110) [4,5], 60 kJ mol^{-1} on Cu(311) [6], and between 69 and 70 kJ mol^{-1} on Cu(100) [7,8]. The high coverage values are about 12–15 kJ mol^{-1} lower than these. These results found a parallel in studies on unsupported polycrystalline Cu and on a $Cu/ZnO/Al_2O_3$ catalyst [9]. The heat of adsorption of CO was found to be 52 kJ mol^{-1} for both in the coverage range from 3×10^{13} to 1×10^{14} molecule cm^{-2}. The surface of the polycrystalline Cu and of the Cu component of the catalyst therefore appeared to be dominated by the (100) and (110) faces (9).

3. The adsorption and dissociation of H_2O on Cu single crystals and on polycrystalline Cu

Spitzer and Luth [10,11] have studied the interaction of H_2O with Cu(110) and Cu(100). They found that on Cu(110), H_2O adsorbed by electron donation from the oxygen atom, and that the adsorbed H_2O dissociated upon heating between 150 and 175 K [10], producing OH species. No dissociation of the molecularly held H_2O was observed on heating H_2O adsorbed on the Cu(100) surface. Pre-adsorbed oxygen resulted in a lowering of the temperature at which OH species were formed on Cu(110) (10) and, importantly, on Cu(100), it resulted in the dissociation of the adsorbed H_2O [11]. These findings translate readily to the observation of Colbourn et al. [12] that H_2O, which is adsorbed on unsupported polycrystalline copper (produced by H_2 reduction of cupric oxide), dissociates on only a small fraction (7–8%) of the total surface. This clearly indicates structure sensitivity.

4. The adsorption and decomposition of CO_2 on Cu single crystals and on supported Cu catalysts

There is some debate about the exact nature of the structure sensitivity of the decomposition of CO_2 on Cu. Wach and Madix [13] noted that greater than 99% of the CO_2 adsorbed on Cu(110) at 180 K dissociated to CO and surface oxygen. Nakamura et al. [14] and Schneider and Hirschwald [15] also found that CO_2 decomposed on Cu(110). However, Fu and Somorjai [16,17] found that CO_2 did not decompose on Cu(110), but it did on Cu(311). Bonicke et al. [18] have found that CO_2 decomposes on Cu(332), while surprisingly, Taylor et al. [19] found that it decomposed on Cu(100). Since it was generally agreed that CO_2 did not decompose on Cu(111) [20,21], it had been thought that flat surfaces were incapable of decomposing CO_2. Again, these findings can be used to explain the observations of Hadden et al. [22] that CO_2 decomposed on only a small fraction ($\sim 10\%$) of unsupported polycrystalline copper surface and that its decomposition was precursor state mediated, a result which was confirmed by Elliott et al. [23] who showed that the CO_2 decomposed on the Cu(110) face of the Cu component of a $Cu/ZnO/Al_2O_3$ catalyst. The resulting oxidised Cu surface was shown to reconstruct.

5. The adsorption and dissociation of H_2 on Cu single crystals and on supported Cu catalysts

The dynamics of the adsorption and desorption of H_2 on Cu shows little dependence on surface morphology. The adsorption on Cu(110) has been found to have an activation energy between 57 to 60 kJ mol^{-1}, but to be dominated by the need to excite the H_2 molecule into the $v = 1$ state [24–27]. The activation energy for adsorption on Cu(100) has been measured to be 48 kJ mol^{-1} but it is also dominated by the need to be in the $v = 1$ state [28]. The desorption activation energy from Cu(111) is 72 kJ mol^{-1} at low coverage (0.01 monolayer) falling to 64 kJ mol^{-1} at high coverage (0.4 monolayer) [29]. Tabatabaei et al. [30] determined a value of the desorption activation energy of hydrogen from the Cu component of a Cu/Al_2O_3 catalyst of 68 kJ mol^{-1} at low coverage (0.07 monolayer) falling to 64 kJ mol^{-1} at high coverage (0.44 monolayer), suggesting that the surface of the alumina-supported Cu was dominated by the (111) face.

The potential clearly exists for the shift reaction catalysed by $Cu/ZnO/Al_2O_3$ catalysts to be struc-

ture sensitive. The corollary of this is that there is therefore an obvious need for the development of a method, or combination of methods, for the in situ determination of the morphology of the Cu component of $Cu/ZnO/Al_2O_3$ catalysts before, after, and possibly, even during, reaction [31–36]. The Topsoe group have been particularly active in this area in the study of $Cu/ZnO/Al_2O_3$ catalysts. They used EXAFS and combined XRD/EXAFS to obtain in situ structural data and to follow dynamical changes occurring during catalysis [31–33]. They found "significant structural and morphological changes of the Cu metal particles" as a function of the ambient gas mixture. The apparent coordination number for Cu was at its lowest (6.5) in a methanol synthesis gas mixture ($CO/CO_2/H_2$), the conclusion from which was that the reducing tendency of this mixture produced anion vacancies in the ZnO at the Cu/ZnO interface, which allowed the Cu to wet the ZnO [31–35]. In an oxidising synthesis gas mixture ($H_2O/CO/CO_2/H_2$), the apparent coordination number was at its highest (9.5). These changes were reversed upon switching the gas mixture.

The group used the Wulff construction to predict the surface populations of the (111), (110) and (100) faces of the copper as a function of the reducing potential of the ambient gas (in a reducing atmosphere, the (110) face predominated [32]). They incorporated these findings into a dynamic microkinetic analysis of the rates of methanol synthesis from $CO/CO_2/H_2$ mixtures, in which the $CO:CO_2$ ratio changed from 5.7 to 2.7. They obtained a fit to all the data only when they allowed for an increase in the number of Cu sites in the higher $CO:CO_2$ ratio, which they reasoned was due to an increase in the Cu(110) surface [34].

The support appears to play an important role in determining the morphology. Topsoe and Topsoe [36] found no change in the coordination number of Cu in a Cu/SiO_2 catalyst upon changing gas mixtures from $CO/CO_2/H_2$ to $H_2O/CO/CO_2/H_2$. However, using environmental electron microscopy, Gai [37] found that the particle size of Cu, supported on Al_2O_3, doubled in size in changing from an ambient gas of CO (0.2 kPa) to O_2 (0.2 kPa) at 473 K. In addition, the centre of the dispersed oxidised copper particle was shown by EDX to be devoid of Cu. The combination of depth profiling and XPS showed that the Cu diffused through the irreducible (non-wetting) Al_2O_3 substrate. These observations by Gai of oxygen-driven redispersion and dissolution of Cu on/in Al_2O_3 are as yet not accounted for in any dynamical description of the $Cu/ZnO/Al_2O_3$ system.

The situation in respect of determining the morphology of the surface of the Cu in an operating $Cu/ZnO/Al_2O_3$ catalyst is obviously highly complex, and as a result, is unresolved yet. In this paper, we shall use CO infrared (IR) spectroscopy to probe the morphology of the surface of the Cu of a $Cu/ZnO/Al_2O_3$ catalyst (60:30:10 supplied by (ICI)) after a series of well defined pre-treatments: (i) reduction in H_2 (5% H_2 in He, 101 kPa, 25 cm^3 min^{-1}) for 16 h at 513 K, (ii) oxidation by CO_2 decomposition at 285 K followed by reduction in CO at 473 K, (iii) oxidation by CO_2 decomposition followed by reduction in H_2 at 473 K, (iv) pre-reduction in CO, and (v) CO_2 treatment on the CO pre-reduced catalyst and CO re-reduction at 473 K.

6. Experimental

6.1. Microreactor

The multipurpose microreactor has been described in detail elsewhere [38]. It is a single tube reactor (20 cm long, 0.4 cm id) connected via a heated capillary to a mass spectrometer (Hiden Analytical, Warrington, England) capable of following 16 mass continuously with temperature/time.

The microreactor system is capable of a number of in situ measurements. Those used here are: (i) total surface area measurements by N_2 frontal chromatography (FC) at 77 K, (ii) copper metal area measurements by N_2O reactive frontal chromatography (RFC), (iii) isothermal and temperature-programmed reduction (TPR) of the catalyst in hydrogen and carbon monoxide.

6.2. The catalysts

The $Cu/ZnO/Al_2O_3$ catalysts were prepared by sodium carbonate precipitation of mixed nitrate solutions of the metals followed by filtration, washing, drying and calcination. (The catalyst was supplied by

ICI.) Before use, the catalysts were reduced in an H_2/He stream (5% H_2, 25 cm^3 min^{-1}, 101 kPa), raising the temperature from ambient to 513 K at 1 K min^{-1}, and holding the temperature at 513 K for 16 h under the H_2/He stream. The catalyst was then cooled to ambient under the H_2/He stream. Prior to use, the adsorbed surface hydrogen was removed by temperature-programmed desorption in He.

The total surface area of the $Cu/ZnO/Al_2O_3$ (60:30:10) catalyst was 65 m^2 g^{-1} and the copper metal area was 29.8 m^2 g^{-1}.

6.3. Gases

Helium was supplied by Linde and was 99.999% pure. Before use, it was passed through a Chromapack Gas Clean moisture filter. The H_2/He (5% H_2), CO_2/He (10% CO_2), CO/He (10% CO) and N_2O/He (5% N_2O) were obtained from Electrochem. Their quoted purities were 99.999%. They were used direct from the cylinder after passage through a liquid nitrogen-cooled zeolite to remove water.

7. Diffuse reflectance infrared Fourier transform spectroscopy (DRIFTS): equipment and technique

DRIFTS experiments were carried out using a Nicolet Magna-IR550 spectrometer equipped with a mercury cadmium telluride detector, together with a "praying mantis" model, diffuse reflectance attachment (Harrick Scientific) and a Harrick high vacuum chamber diffuse reflectance cell (HVC-DR2 low pressure model), having an IR path length of ~2 cm.

8. Results and discussion

As explained in Section 6, the $Cu/ZnO/Al_2O_3$ catalyst was reduced in a H_2/He stream in situ in the Harrick high vacuum chamber diffuse reflectance cell by temperature programming from ambient to 513 K at 1 K min^{-1} in that stream, holding the temperature of the catalyst at 513 K, under H_2/He stream for 16 h. The hydrogen adsorbed on the surface of the catalyst was then desorbed by temperature programming in a He stream. The hydrogen desorption spectrum so produced has been published earlier [39]. The H:Cu surface atom ratio obtained by this method was ~0.2 [39].

Carbon monoxide was dosed on to this catalyst at 285 K from a CO/He stream (10% CO, 101 kPa, 25 cm^3 min^{-1}, 15 min). Gas phase and weakly adsorbed CO were removed by flushing the system with He (101 kPa, 25 cm^3, 25 cm^3 min^{-1}, 40 min). This technique ensured that CO molecules bound to the surface of the Cu with heats of adsorption < 90 kJ mol^{-1} would have been desorbed. Since the heats of adsorption of CO on Cu(111), Cu(110) and Cu(100) are maximally 50, 60 and 70 kJ mol^{-1}, respectively [2–5,7,8], these surfaces will be completely free of any adsorbed CO. The IR spectrum of the CO remaining on the surface is shown in Fig. 1 (spectrum (a)).

One main band is observed at 2100 cm^{-1}. This is identical to that observed for CO adsorbed on Cu dispersed on SiO_2 powder [40–42], but lower than that found for CO adsorbed on Al_2O_3-supported Cu [40,42]. Table 1 lists the frequencies of CO adsorbed on several single crystal faces of Cu.

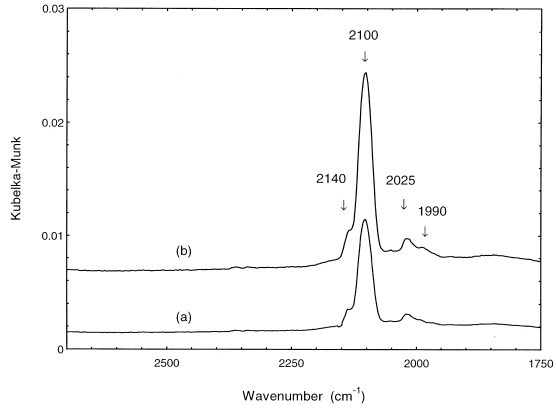

Fig. 1. (a) The IR spectrum of CO adsorbed on the Cu surface produced by H_2 reduction of the polycrystalline copper oxide component of an industrial $Cu/ZnO/Al_2O_3$ catalyst, ICI. (b) The CO IR spectrum of CO adsorbed on the Cu surface produced by (i) H_2 reduction, (ii) CO_2 decomposition at 285 K, and (iii) CO reduction at 473 K of the CO_2 oxidised Cu. (In both Fig. 1a and b the CO IR spectra were taken after having flushed the CO-dosed Cu for 40 min in an He flow, ensuring that all the desorption of CO from the Cu(111), (110) and (100) surfaces.)

Table 1
Frequencies of CO adsorbed on Cu single crystal surfaces

Crystal face	Wave number/cm^{-1}	Reference
Cu(100)	2085	43
Cu(111)	2076	40
Cu(110)	2093	40
Cu(211)	2100	40
Cu(311)	2102	40
Cu(755)	2098	40

The absence of these frequencies for CO adsorbed on SiO_2- or Al_2O_3-supported Cu caused Pritchard to arrive at the unlikely conclusion that the (111), (110) and (100) faces of Cu were conspicuous by their absence from the surface of polycrystalline Cu and that its surface comprised mainly the (211), (311) and (755) surfaces.

This lack of observation of the vibrational frequencies of CO adsorbed on the low index faces of Cu in these studies [40–42], even though the spectra were taken with CO in the cell, was rationalised by Hollins [44]. His explanation was that, where CO is adsorbed on a surface comprising (111) terraces, but which also has steps or defects, dipolar coupling will result in frequency transfer from the lower frequency sites (molecules adsorbed on the terraces) to higher frequency sites (molecules adsorbed on steps) [44].

This cannot be the case here. The spectra are taken in the absence of gas phase CO; in addition the (111), (110) and (100) surfaces of Cu are completely free of any adsorbed CO by having been flushed in a He stream for 40 min at 285 K. Therefore, there can be no intensity transfer from CO adsorbed on the lower index planes to CO adsorbed on the steps. The sharp CO vibrational peak at 2100 cm^{-1} shown in Fig. 1a is therefore that of CO adsorbed on the (211) face of Cu [40]. Furthermore, the intensity of peak is directly proportional to the amount of CO adsorbed on this surface and is thus a measure of the population of the Cu(211) face on the copper surface of the $Cu/ZnO/Al_2O_3$ catalyst.

Raising the temperature from 285 to 513 K in the He stream resulted in the loss of the 2100 cm^{-1} at $\sim$350 K. In a previous study, in which we used CO temperature-programmed desorption to probe the surface morphology of the Cu, we found a high temperature CO desorption state, having a peak maximum temperature of 345 K [45]. The desorption activation energy corresponding to this peak maximum temperature is 101 kJ mol^{-1}, which is greater than the 90 kJ mol^{-1}, which, we calculated, was required for this state to persist on the surface of the catalyst after the 40-min He flush. This, and the near identity of its desorption peak maximum (345 K) and the temperature of the loss of the 2100 cm^{-1} band (350 K), confirms our previous tentative assignment of the 345 K desorption peak as deriving from CO adsorbed on Cu(211).

The amount of CO we measured in this desorption peak was 3×10^{18} molecules on 0.5 g of a $Cu/ZnO/Al_2O_3$, whose Cu surface area was measured by N_2O RFC [35] to be 29.8 m^2 g^{-1}. The coverage of the surface copper by this adsorption state is, therefore, 2×10^{13} molecules cm^{-2} or 2% of a monolayer.

The structure of the Cu(211) surface is shown in Fig. 2. It consists of Cu(111) terraces, which are

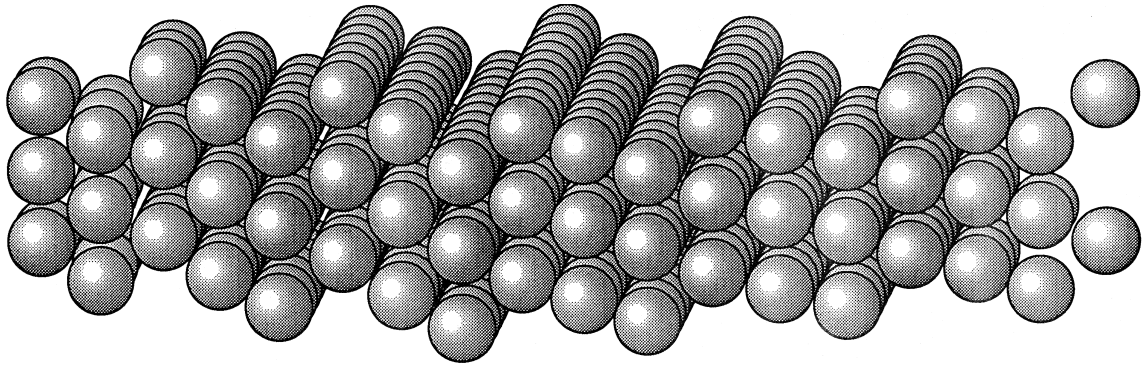

Fig. 2. Structural model of the Cu(211) surface.

three atoms wide with a single Cu(100) step. Since the site for the adsorption of CO on the Cu(211) surface into the high energy desorption state is likely to be atop of the Cu(100) step rather than on the Cu(111) terraces, the total area of the polycrystalline copper surface occupied by the Cu(211) face will be approximately four times the amount of CO desorbing from this state, ~8% of a monolayer. This Cu(211) face is therefore a minority structure on the surface of the polycrystalline copper produced by reduction by hydrogen and desorption of the surface hydrogen.

9. Growth of the Cu(211) surface by CO_2 oxidation followed by CO reduction of the copper

The CO (2×10^{13} molecules (cm^2 Cu)$^{-1}$), which had been adsorbed on to the Cu as described above, was desorbed from the surface of the copper by heating the catalyst to 513 K in a He stream, after which, the temperature was lowered to 285 K in the He stream. The flow was then switched to a CO_2/He stream (10% CO_2, 101 kPa, 25 cm^3 min^{-1}) for 15 min. Previous studies, using mass spectrometric detection (Fig. 3), have shown that this results in the decomposition of the CO_2 and the depositing between 11% and 25% of a monolayer of oxygen atoms on the surface of the copper [23]. This oxidised Cu surface was then reduced in a CO/He (10% CO, 101 kPa, 25 cm^3 min^{-1}) at 473 K for 1 h. The temperature was then lowered to 285 K and the CO/He stream was passed for a further 15 min. The flow was then switched to He and the system was purged for a further 40 min, after which, the CO IR spectrum shown in Fig. 1b was recorded.

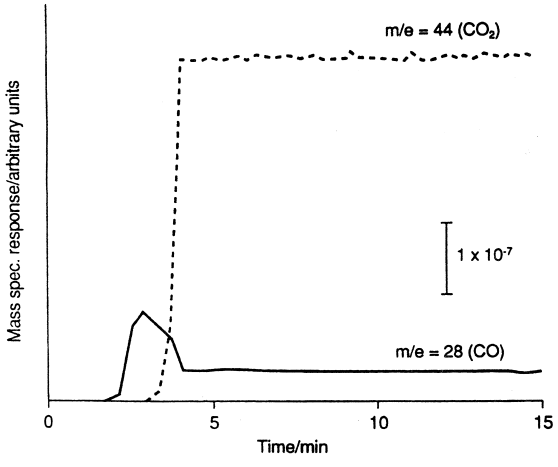

Fig. 3. The decomposition of CO_2 on the Cu surface produced by H_2 reduction of the polycrystalline copper oxide component of the $Cu/ZnO/Al_2O_3$ catalyst.

Again, only one sharp band at 2100 cm^{-1} is observed. Its intensity, however, has increased by a factor of 1.8, so that the surface population of the Cu(211) surface has now become ~20% of the total area. This is completely consistent with the results of our previous thermal desorption study [45]. There, we found after oxidation, the copper by reaction with CO_2 at 213 K, followed by reduction in CO at 473 K and then, CO dosage at 77 K; there was a fivefold increase in the CO desorption state, having a peak maximum temperature of 345 K. The increases in the CO adsorption state having the 2100-cm^{-1} vibrational frequency and in the CO desorption state having a peak maximum temperature of 345 K is additional evidence that they are the same state and that, therefore, the 345 K CO desorbing state is that of CO desorbing from Cu(211).

There are three smaller bands in Fig. 1a and b at 1990, 2025 and 2140 cm^{-1}. The band at 1990 cm^{-1} is hardly visible in Fig. 1a, but appears as a shoulder on the 2025 cm^{-1} band in Fig. 1b. Attribution of the origin of these two lower frequency bands is difficult. Hollins [44] has seen a band at 2040 cm^{-1}, which moved to 2030 cm^{-1}, with increasing coverage when a $^{12}CO/^{13}CO$ (25:75) mixture was adsorbed on Cu (16,15,0). Its origin, however, was never assigned.

The band at 2140 cm^{-1} is probably CO-adsorbed on an oxidised Cu surface, all CO bands above 2100 cm^{-1} being due to CO adsorption on an oxidised Cu surface [44].

10. The effect of subsurface hydrogen in determining the surface morphology of the copper

The growth of the Cu(211) face upon reduction of the partially oxidised surface of the copper by CO at 473 K shows quite clearly that removal of the surface oxygen by CO does not result in the copper

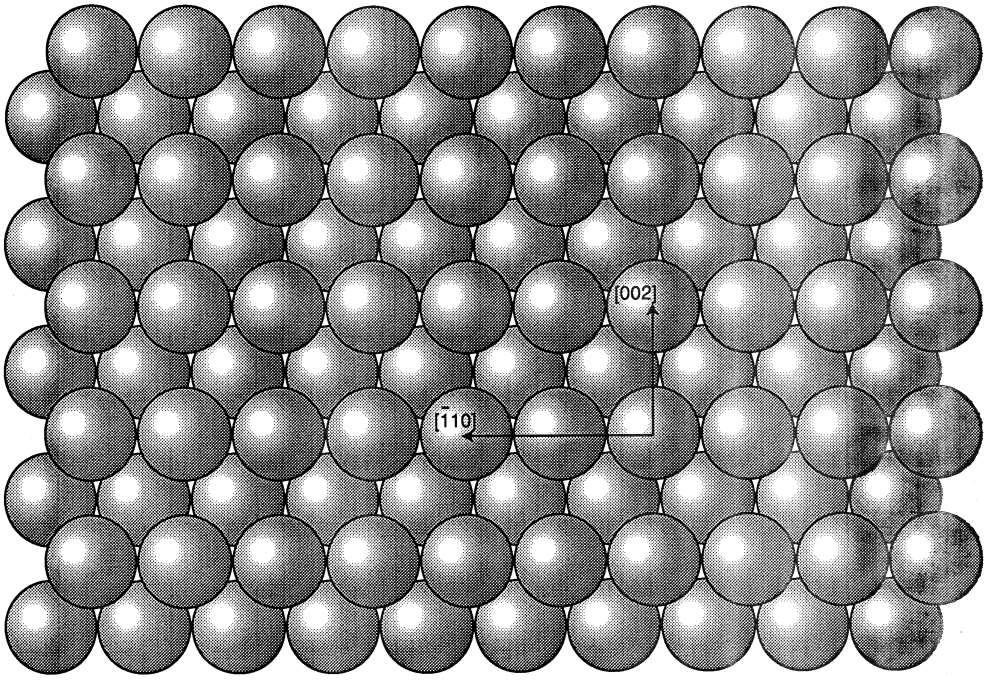

Fig. 4. Structural model of the Cu(110) surface.

surface relaxing back to its original morphology. The initial morphology of the surface of the copper after, firstly, reduction in H_2, and secondly, desorption of the adsorbed surface hydrogen, is determined by the subsurface hydrogen [45].

Single crystal studies have shown that CO_2 decomposition occurs on the (110) and (311) surfaces of copper [14–17]. Partial oxidation of the Cu(110) surface (Fig. 4) has been shown to result in a restructuring of the Cu(110) surface to the (2×1) O–Cu structure shown in Fig. 5 by growth of CuO rows along the $< 002 >$ direction [46]. In our thermal desorption study, we found that removal of the surface oxygen atoms from this structure by reaction

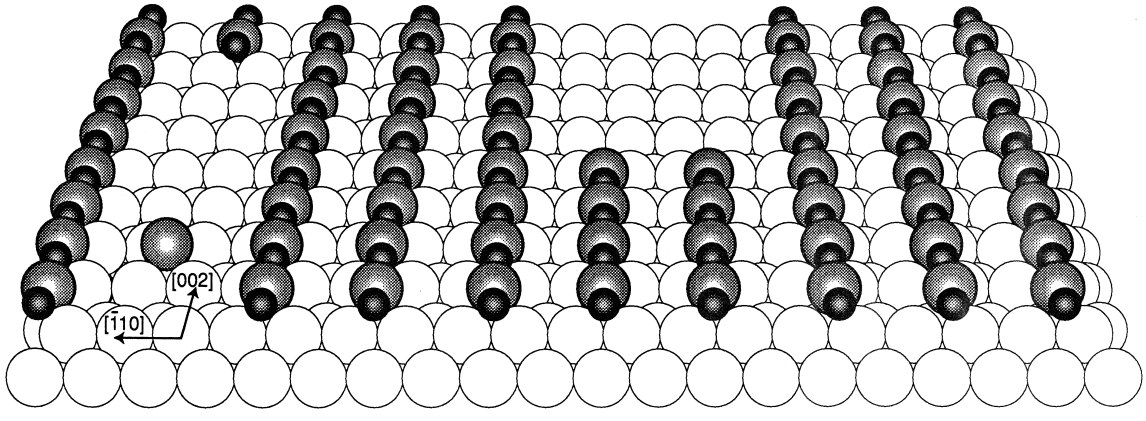

Fig. 5. Structural model of the (2×1) O–Cu surface produced by oxygen adsorption driven reconstruction of Cu(110) [46].

with CO at 473 K did not result in a relaxation of the copper atoms to the original Cu(110) surface [45]. It can be seen from Figs. 2 and 5 that after removal of the oxygen atoms from the (2×1) O–Cu structure (Fig. 5), the Cu(211) surface can be readily produced with minimal movement of the Cu atoms.

The sequence of experiments described below, which were performed (i) on a CO pre-reduced, and (ii) on a H_2 pre-reduced catalyst, demonstrates the crucial importance of hydrogen in determining reactive surface morphology.

11. Reduction in CO, followed by dosing CO_2

Fig. 6 is the TPR profile obtained by heating a fresh sample of the $Cu/ZnO/Al_2O_3$ in a CO/He stream (10% CO, 101 kPa, 25 cm^3 min^{-1}) from ambient to 513 K at 5 K min^{-1}. The loss of the CO is exactly mirrored by the production of the CO_2, the amount of which is quantitative for the reduction of the copper oxide. To ensure complete reduction, the catalyst was held at 513 K, under the CO/He stream for 16 h. The flow was then switched to He and the temperature was lowered to ambient. Fig. 7a is the IR spectrum obtained by passing a CO_2/He stream (10% CO_2, 101 kPa, 25 cm^3 min^{-1}) over the CO-reduced catalyst for 15 min at 285 K, the spectrum being taken at the end of the 15-min dosing time. It is the IR spectrum of gas phase CO_2. Gas phase CO_2 has bands at 2129.5, 2107.3, 2093.6, 2077.3, ~2060

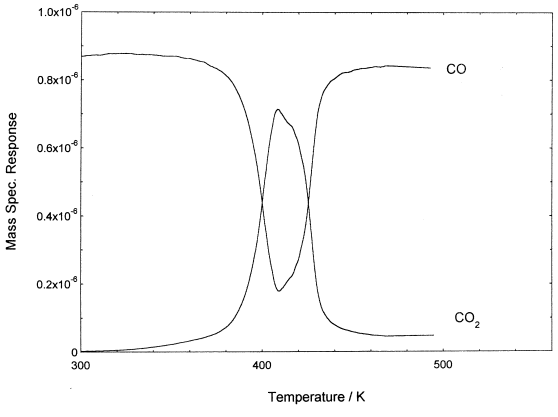

Fig. 6. The temperature-programmed reduction profile produced by reducing the copper oxide component of a $Cu/ZnO/Al_2O_3$ catalyst in a CO/He stream (10% CO, 101 kPa) by raising the temperature from ambient to 513 K at 5 K min^{-1} in that stream.

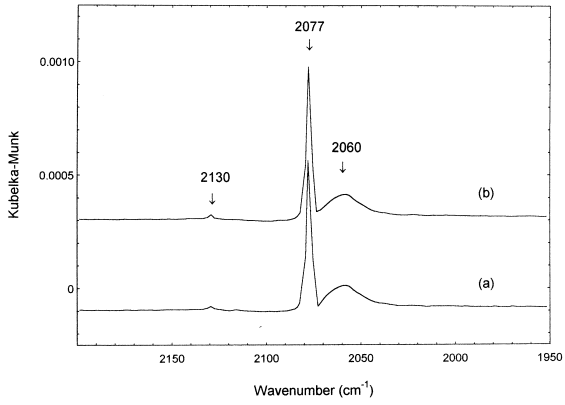

Fig. 7. (a) IR spectrum obtained by passing CO_2/He (10% CO_2, 101 kPa, 25 cm^3 min^{-1}) at 285 K over a CO reduced $Cu/ZnO/Al_2O_3$ catalyst. The spectrum is taken in the CO_2/He gas mixture and is that of gas phase CO_2. (b) IR spectrum obtained by passing the CO_2/He stream over the CO re-reduced sample, at 473 K, of the catalyst treated as described in Fig. 7a. The spectrum is taken in the CO_2/He gas mixture and is again that of gas phase CO_2.

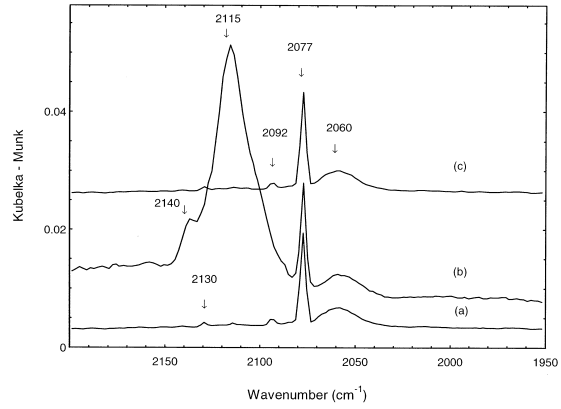

Fig. 8. (a) The IR spectrum produced by passing CO_2/He (10% CO_2, 101 kPa) at 285 K over a H_2 reduced $Cu/ZnO/Al_2O_3$ catalyst. The spectrum is taken in the CO_2/He gas mixture. Note the appearance of bands at 2092 and 2115 cm^{-1}, which are absent in Fig. 7a and b. (b) The IR spectrum produced by passing the CO_2/He stream at 285 K over the CO re-reduced (473 K) catalyst, treated as described in Fig. 8a. The spectrum is taken in the CO_2/He gas mixture. Note the significant growth of the band at 2115 cm^{-1} not seen in Fig. 7b. (c) The IR spectrum produced by passing the CO_2/He mixture at 285 K over the catalyst, treated as described in Fig. 8b, but now having been re-reduced in H_2 at 473 K. The spectrum is taken in the CO_2/He gas mixture. It is identical to that shown in Fig. 8a, demonstrating the hydrogen-driven reconstruction to the original morphology.

(the P branch), 1933, ~1920 and 2037.2 cm^{-1} ($^{13}C^{16}O_2$) [47]. The absence of a band at 2092 cm^{-1} observed in Fig. 7a is extremely important. It is clear from this that the appearance of this band at 2092 cm^{-1} in Fig. 8 from the same CO_2 stream cannot be due to gas phase CO_2.

A second treatment of temperature programming in the CO/He stream, followed by dosing the CO_2/He stream for 15 min at 285 K produced the spectrum shown in Fig. 7b — again that of gas phase CO_2.

12. Reduction in H_2, followed by dosing CO_2

Fig. 8a is the IR spectrum produced by dosing the CO_2/He stream (10% CO_2, 101 kPa, 25 cm^3 min^{-1}) at 285 K for 15 min on to a fresh sample of the Cu/ZnO/Al_2O_3 catalyst, which had been pre-reduced in the H_2/He stream and which had had the adsorbed hydrogen atoms removed from it by temperature-programmed desorption, as described in Section 6. The bands at 2060, 2077 and 2130 cm^{-1} are identical to those seen in Fig. 7a and b and are those of gas phase CO_2. The small bands at 2092 and 2115 cm^{-1} are not seen in Fig. 7. They are those of adsorbed CO deriving from the decomposition of the CO_2 on the Cu. The Cu surface, produced by CO reduction of the copper oxide component of the Cu/ZnO/Al_2O_3 catalyst, does not decompose CO_2.

The band at 2092 cm^{-1} is identical to that found by Pritchard et al. [40] for CO adsorbed on Cu(110), while that at 2115 cm^{-1} is that of CO adsorbed on oxidised Cu — possibly adsorbed on the (2×1) O–Cu surface shown in Fig. 5.

Reduction of this surface oxidised Cu by CO at 473 K and then re-dosing the CO_2/He stream for 15 min produces the spectrum shown in Fig. 8b. The spectrum shows a massive increase in the 2115 cm^{-1} band — CO adsorbed on oxidised Cu — and a loss in the band at 2092 cm^{-1}. This replicates our previous time-dependent CO_2 IR spectra on an H_2-reduced Cu/ZnO/Al_2O_3 catalyst, where we saw a loss of the 2092 cm^{-1} band and a gain in the 2115 cm^{-1} band [23] and confirms the conclusions of our CO temperature-programmed study of morphology, namely that the CO_2 oxidation of the copper occurs on the (110) surface, transforming it to a state which we described as an oxidised Cu(211) surface. (The band at 2140 cm^{-1} is the same as that found in Fig. 1a and b and is probably CO-adsorbed on an oxidised Cu surface different from that giving rise to the 2115 cm^{-1} band.)

H_2 re-reduction of the surface-oxidised copper of Fig. 8b and exposure of the H_2 re-reduced surface to the CO_2/He stream (10% CO_2, 101 kPa, 25 cm^3 min^{-1}) for 15 min produces the spectrum shown in Fig. 8c. The spectra shown in Fig. 8a and c are identical. The original morphology is completely restored.

We have measured the surface oxygen coverage of the Cu component of a Cu/ZnO/Al_2O_3 catalyst, which had been producing methanol from $CO/CO_2/H_2$ feeds of different $CO:CO_2$ ratios. Even though the H_2 was in excess (~80%) of the feed, the oxygen coverage was found to be a function of the $CO:CO_2$ ratio, showing that CO was a better reducing agent than H_2 [48].

Therefore, if the arguments deriving from the use of the Wulff construction held that a more reduced surface should contain a higher surface population of the Cu(110) face [34], then, CO reduction should result in an increase in the surface population of the Cu(110) face. This, therefore, should produce an increase in the extent of CO_2 decomposition. The total absence of any evidence of CO_2 decomposition observed here throws doubt on the method of the Wulff construction reported earlier [34].

13. Conclusions

(1) Hydrogen reduction of the polycrystalline copper oxide component of an ICI Cu/ZnO/Al_2O_3 catalyst produces a surface morphology of Cu, which is active in the decomposition of CO_2. This surface has been shown to comprise the Cu(110) face and the minority Cu(211) face.

(2) CO reduction at 473 K of the copper surface, which had been oxidised by CO_2 decomposition at 285 K, resulted in a twofold increase in the surface population of the Cu(211) face.

(3) H_2 reduction at 473 K of the copper surface, which had been oxidised by CO_2 decomposition at

285 K, resulted in a restoration of the original morphology.

(4) CO reduction of the polycrystalline copper oxide component of an ICI $Cu/ZnO/Al_2O_3$ catalyst produces a surface morphology of Cu, which is inactive in the decomposition of CO_2. This is in complete contrast to the surface morphology of the Cu produced by H_2 reduction of the polycrystalline copper oxide component of the $Cu/ZnO/Al_2O_3$ catalyst.

References

[1] R.A. Hadden, P.J. Lambert, C. Ranson, Appl. Catal. 122 (1995) L1–L4.
[2] J. Kessler, K. Thieme, Surf. Sci. 67 (1977) 405.
[3] P. Hollins, J. Pritchard, Surf. Sci. 89 (1979) 486.
[4] C. Harandt, J. Gosehnick, W. Hirschwald, Surf. Sci. 152/153 (1987) 453.
[5] K. Horn, M. Hussain, J. Pritchard, Surf. Sci. 63 (1977) 244.
[6] H. Papp, J. Pritchard, Surf. Sci. 53 (1975) 371.
[7] J.C. Tracy, J. Chem. Phys. 56 (1972) 2748.
[8] C.M. Troung, J.A. Rodriguez, D.W. Goodman, Surf. Sci. 271 (1992) L385.
[9] K.C. Waugh, Appl. Catal. 43 (1988) 315.
[10] A. Spitzer, H. Luth, Surf. Sci. 120 (1982) 376.
[11] A. Spritzer, H. Luth, Surf. Sci. 152/153 (1985) 543.
[12] E. Colbourn, R.A. Hadden, H.D. Vandervell, K.C. Waugh, G. Webb, J. Catal. 130 (1991) 514.
[13] I.E. Wach, R.J. Madix, J. Catal. 53 (1978) 208.
[14] J. Nakamura, J.A. Rodrigues, C.T. Campbell, J. Phys.: Condens. Matter 1 (1989) SB149.
[15] T. Schneider, W. Hirschwald, Catal. Lett. 14 (1992) 192.
[16] S. Fu, G.A. Somorjai, Surf. Sci. 237 (1990) 87.
[17] S. Fu, G.A. Somorjai, Surf. Sci. 262 (1992) 68.
[18] I.A. Bonicke, W. Kirstein, F. Thieme, Surf. Sci. 177 (1994) 307.
[19] P.A. Taylor, P.B. Rasmussen, I. Chorkendorff, J. Vac. Sci. Technol., A 10 (1992) 2750.
[20] C.T. Campbell, K.A. Daube, J.M. White, Surf. Sci. 137 (1987) 458.
[21] F.H.P.M. Habraken, E. Kieffer, G.A. Bootsma, Surf. Sci. 83 (1979) 333.
[22] R.A. Hadden, H.D. Vandervell, K.C. Waugh, G. Webb, Catal. Lett. 1 (1988) 27.
[23] A.J. Elliott, R.A. Hadden, J. Tabatabaei, K.C. Waugh, F.W. Zemicael, J. Catal. 157 (1995) 153–161.
[24] J.M. Campbell, C.T. Campbell, Surf. Sci. 259 (1991) 1.
[25] B.E. Hayden, C.L.A. Lamont, Chem. Phys. Lett. 160 (1989) 331.
[26] B.E. Hayden, C.L.A. Lamont, Chem. Phys. Lett. 63 (1989) 1823.
[27] B.E. Hayden, D. Lakey, J. Schott, Surf. Sci. 239 (1990) 119.
[28] P.B. Rasmussen, P.M. Holmblad, H. Christoffersen, P.A. Taylor, I. Chorkendorff, Surf. Sci 287/288 (1993) 79.
[29] G. Anger, A. Winkler, K.D. Rendulic, Surf. Sci. 220 (1989) 1.
[30] J. Tabatabaei, B.H. Sakakini, M.J. Watson, K.C. Waugh, Catal. Lett. 59 (1999) 143.
[31] B.S. Clausen, G. Steffensen, B. Fabius, J. Villadsen, R. Feidenhans'l, H. Topsoe, J. Catal. 132 (1991) 524.
[32] B.S. Clausen, J. Schiotz, L. Grabaek, C.V. Ovesen, K.W. Jacobsen, J.K. Norskov, H. Topsoe, Top. Catal. 1 (1994) 367.
[33] B.S. Clausen, L. Grabaek, G. Steffensen, P.L. Hansen, H. Topsoe, Catal. Lett. 20 (1993) 23.
[34] C.V. Ovesen, B.S. Clausen, J. Schiotz, P. Stoltze, H. Topsoe, J.K. Norskov, J. Catal. 168 (1997) 133.
[35] H. Topsoe, C.V. Ovesen, B.S. Clausen, N.-Y. Topsoe, P.E.H. Nielsen, E. Tornqvist, J.K. Norskov, in: G.F. Froment, K.C. Waugh (Eds.), Dynamics of Surfaces and Reaction Kinetics in Heterogeneous Catalysis, Elsevier, Amsterdam, 1997, p. 121.
[36] N.-Y. Topsoe, H. Topsoe, Top. Catal. 8 (1999) 267.
[37] P.L. Gai, Top. Catal. 8 (1999) 97.
[38] G.C. Chinchen, C.M. Hay, H.D. Vandervell, K.C. Waugh, J. Catal. 103 (1987) 79.
[39] S. Bailey, K.C. Waugh, Catal. Lett. 17 (1993) 371.
[40] J. Pritchard, T. Catterick, R.K. Gupta, Surf. Sci. 53 (1975) 1.
[41] R.P. Eischens, W.A. Pliskin, Adv. Catal. 10 (1958) 1.
[42] A.W. Smith, J.M. Quets, J. Catal. 4 (1965) 163.
[43] M.A. Chesters, J. Pritchard, M.L. Sims, in: F. Ricca (Ed.), Adsorption Desorption Phenomena, Academic Press, London, 1972, p. 277.
[44] P. Hollins, Surf. Sci. 16 (1992) 54.
[45] R.A. Hadden, B. Sakakini, J. Tabatabaei, K.C. Waugh, Catal. Lett. 44 (1997) 145.
[46] D.J. Coulman, J. Winterlin, R.H. Behm, G. Ertl, Phys. Rev. Lett. 64 (1990) 1761.
[47] I. Gausemel, O.H. Ellestad, C.J. Nielsen, Catal. Lett. 45 (1997) 129.
[48] G.C. Chinchen, K.C. Waugh, D.A. Whan, Appl. Catal. 25 (1986) 101.